JOURNAL OF OPTOELECTRONICS AND ADVANCED MATERIALS Vol. 9, No. 8, August 2007, p. 2566 - 2570

Structural characterization of yttrium silica sol-gel microspheres

D. CACAINA[a,b], R. V. F. TURCU[a], D. A. UDVAR[a], M. VAAHTIO[b], H. YLÄNEN[b], S. SIMON[a]
[a]*Babes-Bolyai University, Faculty of Physics, M. Kogalniceanu 1, Cluj-Napoca, 400084, Romania.*
[b]*University of Turku, Turku Biomaterials Centre, Itäinen Pitkäkatu 4 B (PharmaCity),Turku, FIN-20520, Finland*

Sol-gel silica microspheres incorporating yttrium were prepared and structural investigated as possible carrier materials for the radiation inside the cancer tumours. The studied microspheres were obtained by sol-gel and spray-drying methods and thermally treated in order to control the chemical stability of the samples in the human body environment. Several methods were used for structural characterization of the microspheres. The shape and composition of silica microspheres was investigated by Back Scattered Electron Imaging of Scanning Electron Microscope equipped with Energy Dispersive X-ray Analysis (EDXA). Laser Ablation Inductively Coupled Plasma Mass Spectrometry (LA-ICP-MS) was used for the analysis of the distribution of yttrium in the materials. Information about the local structure of the samples was obtained by Nuclear Magnetic Resonance (NMR) Spectroscopy on ^{29}Si nucleus. The results show that yttrium was well incorporated in some of the silica microspheres and the local structure of the samples is influenced by the incorporation of yttrium into the silica network.

(Received March 5, 2007; accepted June 1, 2007)

Keywords: Sol-gel, Yttrium, Local structure, SEM, EDXA, LA-ICP-MS

1. Introduction

Biodegradable and non-biodegradable beta-emitting microspheres have been widely investigated for the use as carrier material for the radiation inside the cancer tumours, in order to provide a high and localized dose of beta radiation [1-3]. The sol-gel process based on the hydrolysis and condensation of silicon alkoxides compounds, has various medical applications such as the formation of bioactive glass and thin coatings [4,5].

The sol-gel method allows preparing high purity and homogeneity materials at relative low temperatures. New generation of ceramic materials with great structural properties has emerged with the sol-gel processing due to the possibility of manipulation and control of the nanostructures. The possibility of obtaining non-crystalline materials with controlled composition and structures makes the sol-gel processing a potential technique for the encapsulation of isotopes for therapeutic applications. The high porosity and surface area associated with the typical structure of the xerogel produced by sol-gel allow obtaining materials with different degradation rate [2,6,7]. By spray-drying, sol-gel microspheres with desired size can be obtained [8,9].

The aim of this study was to manufacture by sol-gel and spray-drying methods biodegradable silica microspheres containing yttrium and to investigate their structure by several techniques.

BEI-SEM/EDX analysis revealed the surface properties of the prepared microspheres and the incorporation of yttrium in the microspheres. The incorporation of yttrium in the silica network is expected to induce changes in the local structure and to influence the properties of the materials. NMR spectroscopy provides valuable information on the structural units that are forming the glass network and is sensitive to changes in the composition of the materials. Q^n terminology is used to describe the structure of silicate glasses, where n is the number of bridging oxygens in a SiO_4 group [10]. The structural units are well identified in silicate systems by ^{29}Si MAS-NMR spectroscopy.

2. Experimental

Silica rich microspheres of less than 50 μm of diameter incorporating yttrium were prepared by sol-gel and spray-drying methods. The investigated samples contain 16.6 wt% yttrium oxide. The sols were obtained by the hydrolysis and polycondensation of tetraethoxysilane (TEOS) and yttrium (III) nitrate hexahydrate ($Y(NO_3)_3 \cdot 6\ H_2O$), that have been used as precursors. The nitrate was dissolved in water and hydrochloric acid was used as the catalyst. Different H_2O/TEOS ratios were used in order to obtain microspheres with suitable properties for the proposed application. For the SiY12 sample, ethanol was added to the sol in a ratio TEOS/EtOH 1:7. The sol-gel formulation and spray-drying parameters for the four selected samples are given in Table 1.

Table 1. The sol-gel and spray-drying parameters.

Sample	Sol-gel formulation				Spraying parameters			
	R_1	R_2	pH_f	r	P (%)	A (%)	F (l/h)	T_i (^{0}C)
SiY05	22	30	1.7	0	16	95	400	150
SiY06	30	38	2.0	0	16	95	400	150
SiY09	61	91	3.3	0	16	95	400	170
SiY12	61	91	3.6	7:1	16	95	400	170

R_1-initial H_2O/TEOS ratio, R_2-final H_2O/TEOS ratio, pH_f-final pH, r-EtOH/TEOS ratio, P-pump, F-flow, A-aspirator, T_i-inlet temperature.

The microspheres were obtained by spraying yttrium silica hydrolysed sols with a Buchi-191 mini spray dryer. Several yttrium silica samples were prepared in order to optimise the processing parameters. The obtained microspheres were thermally treated at 700 ^{o}C for 2 hours.

The incorporation of yttrium in the obtained microspheres was analysed by BEI-SEM. EDX analysis was used for elemental analysis of the composition of the microspheres. The distribution of yttrium in the material was investigated by LA-ICP-MS. The measurements were carried out using powder pellets. The spot size for the analysis was 6 μm.

The local structure of the samples was evaluated by ^{29}Si MAS-NMR. All the NMR samples spectra were collected using a full digital BRUKER Avance 400 UltraShield^{TM} spectrometer, with superconductor magnet of 9.4 T magnetic field. ^{29}Si NMR chemical shifts are expressed in ppm relative to an 1% $Si(CH_3)_4/CDCl_3$. The experiments have been made with spinning speed of 6 kHz.

3. Results and discussion

The surface properties of the sol-gel and spray-dried microspheres and the incorporation of yttrium in the microspheres were investigated by BEI-SEM/EDXA. The SEM results show that the obtained particles are hollow and have a spherical shape with a diameter of less than 50 μm. The microspheres are hollow due to the well-dispersed sol obtained by the sol-gel formulation used.

During the spray-drying of well-dispersed sols, a gel layer initially forms at the surface of the drops due to rapid evaporation of water from the drop's surface. This gel layer is semi-permeable to water/vapour flow and reduces the rate of evaporation of the solvent. The calculations for the net interaction potential between the colloidal aggregates indicate that the barrier-to-aggregation in this sol is relatively high [11]. Hence, gelation occurs by a reaction-limited process, producing a relatively dense microporous gel layer with correspondingly low permeability. The reduced evaporation rate through the gel layer results in a temperature increase, which at a high inlet temperature leads to "ballooning". At a low inlet temperature, the well-dispersed colloids in the drops remain relatively mobile as water evaporates through the gel layer at the surface of the drop, producing a diffusion-gradient towards the surface. As liquid flows to the drop surface, with accompanying solids, a gradual growth of the solid shell occurs, leaving a void in the centre of the particle [11].

Four mechanisms leading to the formation of hollow granules have been reported [12]: (1) ballooning, where the internal pressure causes the droplet to expand; (2) moisture evaporating at a faster rate than the diffusion of solids back into the droplet interior, leaving air voids; (3) suspended solids being drawn to the droplet surface as liquid migrates because of capillary action; and (4) entrained air in the feed slurry persisting as voids.

Apart from the effect of the drying rate, the shell thickness varies with the solid concentration of the sprayed-dried feed stock. Dilute sols produce thin-walled particles while concentrated sols yield thick-walled particles.

Figs. 1 to 3 shows the BEI-SEM images of two of the selected samples, SiY05 and SiY12. As can be observed, in the SiY05 sample (Fig. 1) the microspheres are stuck to each other. EDX analysis on this sample indicated the presence of yttrium not only inside of the microspheres but also on their surface. This could contribute to the sticky property of the powder. The microspheres belonging to the SiY06 sample exhibit almost the same feature.

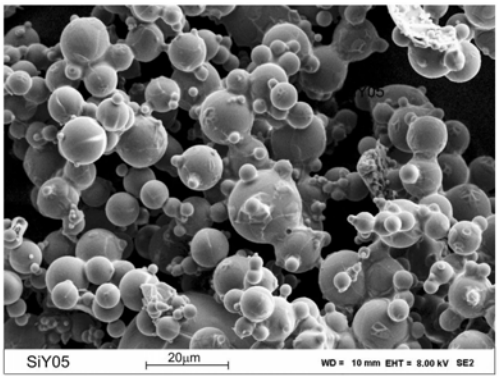

Fig. 1. BEI-SEM micrograph of SiY05 microspheres.

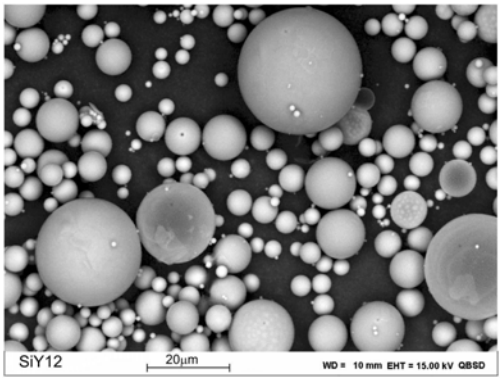

Fig. 2 BEI-SEM micrograph of SiY12 microspheres.

SEM micrographs of the SiY09 and SiY12 (Fig. 2) show well-defined microspheres with no detectable yttrium on their surface, as EDX analysis reveals. The SEM image of the one microsphere belonging to the SiY12 sample reveals the distribution of yttrium in the silica network (Fig. 3). It can be observed the presence of small yttrium clusters of nanometer sizes which are homogeneously encapsulated in the silica network. Hence, yttrium is encapsulated in the network rather than forming part of the molecular structure.

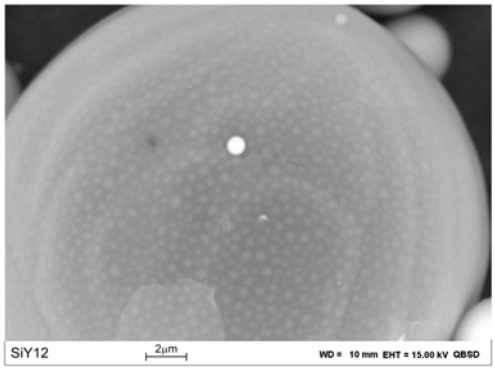

Fig. 3. BEI-SEM micrograph of one of the SiY12 microsphere.

Several microspheres with different diameters from each sample were randomly selected and the concentration of yttria and silica was measured by EDX analysis. The EDX results presented in Table II indicate that for the SiY09 and SiY12 samples, the concentration of yttrium oxide and silica is close to the theoretical concentration.

SEM/EDXA results indicate that an increase of the H_2O/TEOS ratio leads to a better incorporation of yttrium in the silica microspheres. Moreover, the addition of ethanol to the composition contributes to a well incorporation of yttrium and improves the surface properties of the microspheres. The increase of H_2O/TEOS ratio leads to obtaining thin-walled particles due to the highly diluted and well-dispersed sol. The thickness of the wall particles depends also on the size of the microspheres. The small microspheres have thicker walls than the bigger microspheres.

Table 2. Theoretical and experimental concentrations as determined by SEM/EDXA.

Sample	$(SiO_2)_{th}$	$(SiO_2)_{ex}$	$(Y_2O_3)_{th}$	$(Y_2O_3)_{ex}$
SiY05	83.4	85.76	16.6	14.24
SiY06		87.36		12.64
SiY09		84		16
SiY12		82.15		17.85

The investigated samples were analyzed by LA-ICP-MS in order to gain information about the spatial distribution of yttrium in the prepared materials. The recorded patterns for two of the samples are shown in Figures 4 and 5.

The focusing of the laser beam on the surface of the pellet evaporates a micro-amount of the sample and this micro-amount of the laser-ablated material is transported by a carrier gas to the ICP-MS. This gave the signals as illustrated in the figures. The obtained signals are proportional to the concentration of the analyzed element in the ablated material.

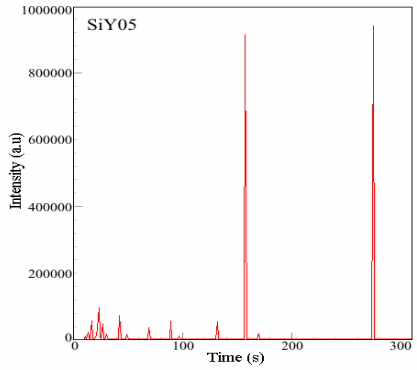

Fig. 4. LA-ICP-MS patterns of the SiY05 sample. Spot size 6 µm and scan speed 10.

As can be observed from the Fig. 4, yttrium is not homogeneously distributed in the SiY05 sample. The high peaks in the spectrum indicate the presence of a high amount of yttrium in those positions; whereas the regions with small or without peaks are poor in yttrium. The results indicate the presence of a high amount of microspheres which do not contain yttrium in the ablated material. In contrast, the patterns of the spectra for the SiY09 sample (Fig. 5) show a quite homogeneous distribution of yttrium in the ablated material. The same results were obtained from the SiY06 and SiY12 samples.

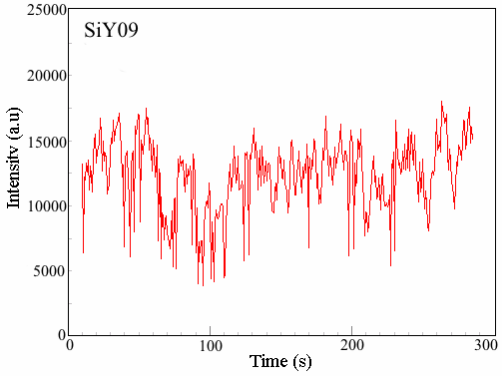

Fig. 5. LA-ICP-MS patterns of the SiY09 sample. Spot size 6 µm and scan speed 5.

MAS-NMR spectroscopy on the ^{29}Si nucleus was used for structural characterization of some selected yttrium silica microspheres thermally treated at 700 ^{o}C. In the Figs. 6 to 9, the ^{29}Si MAS-NMR spectra of the four investigated samples are shown.

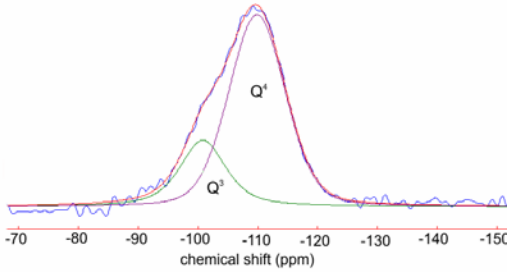

Fig. 6. ^{29}Si MAS-NMR spectra of the SiY05 sample. Experimental and deconvolutions.

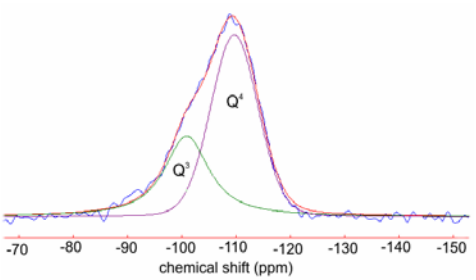

Fig. 7. ^{29}Si MAS-NMR spectra of the SiY06 sample. Experimental and deconvolutions.

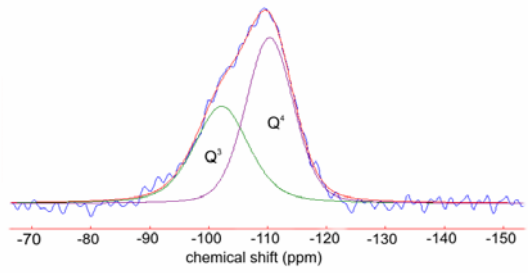

Fig. 8. ^{29}Si MAS-NMR spectra of the SiY09 sample. Experimental and deconvolutions.

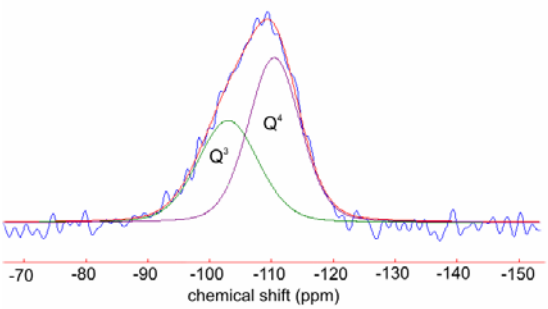

Fig. 9. ^{29}Si MAS-NMR spectra of the SiY12 sample. Experimental and deconvolutions.

The spectra of all the samples consist of a broad and asymmetric resonance line characteristic for amorphous phases. The asymmetry of the line shows the contribution of two peaks to the resonance line. The overlapped signals were deconvoluted using a DMFIT program [13]. The position, line widths and integrated areas of each signal obtained by the deconvolution procedure are summarized in Table 3.

Table 3. Chemical shift, line widths and percent contribution of the two components in the ^{29}Si MAS-NMR spectra of the samples.

Sample	Species	δ (ppm)	fwhm (ppm)	Q (%)
SiY05	Q^3	-100.8	9.1	24.9
(700^0C)	Q^4	-109.9	11.1	75.1
SiY06	Q^3	-100.9	9.9	36.7
(700^0C)	Q^4	-109.7	10.3	63.3
SiY09	Q^3	-102.2	11	42.3
(700^0C)	Q^4	-110.4	9.5	57.7
SiY12	Q^3	-103	11.6	41.9
(700^0C)	Q^4	-110.5	10	58.1

The deconvoluted spectra exhibit one resonance line at ~101 ppm corresponding to Q^3 silicate species and a resonance line at ~110 ppm corresponding to Q^4 units. These chemical shifts typical of highly condensed species may be assigned to O_3Si-OH (or O_3Si-O-Y^{3+}) and O_4Si [7,14-16]. The high number of Q^4 sites is present in the microspheres structure due to the silica polymerization process which involves dehydration and cross-linking during thermal treatment. The Q^3 structure is related to a higher number of -OH groups than the Q^4 structure.

The absence of the resonance line corresponding to Q^2 and Q^1 units shows that no low-condensed silicate species are present in the microspheres' structure after the thermal treatment. This fact indicates that yttrium is not incorporated in the silica network at a molecular level.

The symmetry of the -110 ppm component in the ^{29}Si spectra, attributed to the Q^4 environment, shows that the substitution of silicon atoms by yttrium in neighbouring tetrahedral does not occur. Therefore, we can conclude that there is no direct evidence of Si-O-Y bond formation. Y^{3+} ions could be located in the interstitial positions and surrounded by OH^- ions. The hydrolysed Y^{3+} ions could form yttrium oxide particles upon heating. However, BEI-SEM analysis of the SiY09 and SiY12 samples reveal the presence of small yttrium oxide nanoparticles distributed within the silica network. Moreover, the BEI-SEM results obtained from these samples indicate a better incorporation of yttrium into these microspheres samples

than for the SiY05 and SiY06 samples, where yttrium was found also on the surface of the microspheres.

The Q^4/Q^3 ratio calculated from the deconvolution results shows a decrease from the SiY05 sample to the SiY12 sample. The lowest Q^4/Q^3 ratio was found for the SiY09 and SiY12 samples. The results indicate that the presence of small yttria nanoparticles could hamper the silica polycondensation and distort the silica network. Moreover, the results show that yttrium is encapsulated in the silica network rather than forming part of the network

4. Conclusions

BEI-SEM/EDX analysis provides valuable information about the surface properties and the incorporation of yttrium in the structure of the microspheres.

The structural investigation of the samples indicates that the incorporation of yttrium in the silica microspheres strongly depends on the sol-gel formulation and on the processing parameters.

^{29}Si MAS-NMR results reveal the presence of Q^3 and Q^4 units in the structure of the investigated samples. The proportion of these units in the structure is related to the number of OH groups in the structure and also to the presence of yttrium in the interstitial positions which could hamper the silica polycondensation.

Using the optimal processing parameters, yttrium can be well incorporated and stabilized in silica microspheres prepared by sol-gel and spray-drying methods.

Acknowledgements

Marie Curie Fellowships Program (HPMT-CT-2001-00297) at Åbo Akademi University, Process Chemistry Centre, Turku, Finland and National University Research Council Program CNCSIS (TD 2/32) at Babes-Bolyai University, Faculty of Physics, Cluj, Romania, are acknowledged for the financial support of this work.

References

[1] J. E. White, D. E. Day, Key Engineering Materials **94-95**, 181 (1994).
[2] W. S. Roberto, M. M. Pereira, T. P. R. Campos, Artificial Organs **27**(5), 420 (2003).
[3] J. F. W. Nijsen, A. D. van het Schip, W. E. Hennink, D. W. Rook, P. P. Van Rijk, J. M. H. de Klerk, Current Medicinal Chemistry **1**, 73 (2002).
[4] C. Garcia, S. Cere, A. Duran, J. Non-Cryst. Solids **352** (32-35), 3488 (2006).
[5] J. Jones, P. Sepulveda, L. L. Hench, J. Biomed. Mater. Res. (App. Biomter) **58**, 720 (2001).
[6] D. Cacaina, R. Viitala, M. Jokinen, H. Ylänen, M. Hupa, S. Simon, Key Engineering Materials, **284-286**, 411 (2005).
[7] C. J. Brinker, G. W. Scherer, Sol-gel Science: The Physics and Chemistry of Sol-Gel Processing, Academic Press, New York (1990).
[8] G. Bertrand, P. Roy, C. Filiatre, C. Coddet, Chemical Engineering Science **60**, 95 (2005).
[9] S. L. Lukasiewicz, J. Am. Ceram. Soc. **2** (4), 617 (1989).
[10] R. Viitala, M. Jokinen, S. L. Maunu, H. Jalonen, J. B. Rosenholm, J. Non-Cryst. Solids **351**, 3225 (2005).
[11] E. Sizgek, J. R. Bartlett, M. P. Brungs, J. Sol-gel Science and Technology **13**, 1011 (1998).
[12] W. J. Walker, J. S. Reed, J. Am. Ceram. Soc. **82** (7), 1711 (1999).
[13] D. Massiot, F. Fayon, M. Capron, I. King, S. Le Calve, B. Alonso, J. O. Durand, B. Bujoli, Z. Gan, G. Hoatson, Magn. Reson. Chem. **40**, 70 (2002).
[14] J. Parmentier, K. Liddell, D. P. Thompson, H. Lemercier, N. Schneider, S. Hampshire, P. R. Bodart, R. K. Harris, Solid State Science **3**, 495 (2001).
[15] C. Cannas, M. Casu, A. Lai, A. Musinu, G. Piccaluga, Phys. Chem. Chem. Phys. **4**, 2286 (2002).
[16] J. Parmentier, P. R. Bodart, L. Audoin, G. Massouras, D. P. Thompson, R. K. Harris, P. Goursat, J. L. Besson, J. Solid State Chemistry **149**, 16 (2000).

*Corresponding author: cdana@phys.ubbcluj.ro